Published in final edited form as:
J Proteome Res. 2008 October ; 7(10): 4225–4236. doi:10.1021/pr800044q.

Tissue-Specific Expression and Posttranslational Modification of Histone H3 Variants

Benjamin A. Garcia[†,ζ], **C. Eric Thomas**[‡], **Neil L. Kelleher**[†,‡,*], and **Craig A. Mizzen**[Δ,†,*]

†*Institute for Genomic Biology, University of Illinois at Urbana-Champaign, Urbana, Illinois 61801*

‡*Department of Chemistry, University of Illinois at Urbana-Champaign, Urbana, Illinois 61801*

Δ*Department of Cell and Developmental Biology, University of Illinois at Urbana-Champaign, Urbana, Illinois 61801*

Abstract

Analyses of histone H3 from ten rat tissues using a Middle Down proteomics platform revealed tissue-specific differences in their expression and global PTM abundance. ESI/FTMS with electron capture dissociation showed that, in general, these proteins were hypomodified in heart, liver and testes. H3.3 was hypermodified compared to H3.2 in some, but not all tissues. In addition, a novel rat testes-specific H3 protein was identified with this approach.

Keywords

histone; posttranslational modification; mass spectrometry; electron capture dissociation; variants; proteomic

Introduction

Eukaryotic DNA is complexed with the four core histones, H2A, H2B, H3 and H4 to form nucleosomes, the basic repeating subunit of chromatin.[1] Many studies have highlighted that regulated, dynamic changes in chromatin structure impact DNA-templated processes such as transcription, DNA replication and DNA repair. At the heart of chromatin structure modulation are the covalent posttranslational modifications (PTMs) targeted to histone proteins, including methylation, acetylation, phosphorylation, ubiquitylation and other types of marks.[2] These PTMs occur predominantly at sites clustered within the amino terminal tails of the histones and are thought to influence the dynamics of both tail domain conformation and their interactions with DNA and other proteins. Although the precise function of many of these modifications has not been completely defined, several of these marks have been associated with gene activation or silencing, DNA damage repair and cell cycle progression.[3-11] For example, the trimethylation of lysine 9 on histone H3 (H3K9me3) is enriched in heterochromatic regions of the genome and is linked to gene repression whereas H3K4me3 appears to be selectively enriched at the promoters of active genes and is thought to play a role in transcription initiation.[3,4] Other modifications such as dynamic acetylation of lysines in histones H3 and H4 have also been reported to be associated with transcriptional activation,

*Corresponding authors: (CAM) B107 Chemical & Life Sciences Laboratory, 601 S. Goodwin Ave., Urbana IL 61801, Tel. 217-244-4896; cmizzen@life.uiuc.edu; (NLK) 53 Roger Adams Laboratory, 600 S. Mathews Ave., Urbana, IL 61801, Tel. 217-244-3927; kelleher@scs.uiuc.edu

ζPresent address: (BAG) Department of Molecular Biology, Princeton University, Princeton, NJ 08544; bagarcia@princeton.edu

while phosphorylation of histone H3 at T3, S10 and S28 correlates with the onset of mitosis.[9-11]

The organs and tissues of the human body are comprised by a variety of cell types, all of which have the same genome. Strikingly, although the levels of transcripts from many genes which are expressed ubiquitously varies among different tissues, relatively small numbers of genes are expressed in tissue-specific fashion to contribute to the morphological and biochemical characteristics that distinguish the phenotypes of these cell types.[12-14] These distinct gene expression patterns are typically created during early development in an organism, when cellular differentiation and tissue/organ formation take place. These transcription patterns must be faithfully transmitted throughout cell lineages for normal development to occur, but we are only just beginning to appreciate some of the epigenetic processes which establish and transmit these patterns. Heritable changes in epigenetic mechanisms including DNA methylation, RNA interference and histone modifications are emerging as key factors in determining the gene expression profiles which distinguish different cell types[15,16] and recent data have highlighted important roles for histone modifications in this process. Changes in histone modifications are known to accompany embryonic stem cell differentiation and early embryo development. Lee et al., have demonstrated that histone acetylation and H3K4 methylation levels decrease during embryonic stem cell differentiation *in vitro*.[17] Additionally, they showed that this was accompanied by increased H3K9 methylation, indicating that multiple changes in histone modification are involved in the mechanisms leading to the increased gene silencing and decreased global transcriptional complexity that accompany differentiation. Consistent with these observations, histone deacetylase (HDAC) inhibitors block the differentiation of embryonic cells, reinforcing the importance of global histone acetylation patterns in these cells. Other reports have provided evidence that specific histone modifications may directly modulate developmental regulators involved in embryonic stem cell differentiation.[18-23] For example, Boyer et al., demonstrated that H3K27me3-mediated binding of the Polycomb repressive complexes PRC1 and PRC2 is involved in maintaining embryonic stem cell pluripotency through the repression of a set of 512 genes encoding developmental regulators.[20] Another report also linked K27 methylation with regulating gene expression during skeletal muscle differentiation by showing that expression of the Ezh2 methyltransferase coincided with the activation of muscle-specific genes.[21]

Mass spectrometry (MS) has become a key technique for the analysis of histone PTMs from a wide variety of sources.[24-38] Early MS efforts focused on the confirmation of known histone PTMs and also resulted in the discovery of novel modification sites. More recent studies have attempted to quantify the site occupancy of various histone modifications and compare the differently modified histone forms in samples potentially differing in epigenetic status, such as histones extracted from wild-type and a mouse model of lupus disease.[38-40] Top Down mass spectrometry has been shown to be particularly useful for characterizing combinations of modifications on intact histones or large fragments derived from them,[41-48] and this combinatorial aspect of histone modification has been shown to be biologically significant.[49-51] Given the likely involvement of epigenetic mechanisms in both development and diseases, accurate characterization and quantification of the histone PTMs normally present in various mammalian tissues is of fundamental importance for understanding normal development and the pathogenesis of various diseases. A recent example highlighting the challenges in this endeavor is a report from Mann and co-workers which used tandem mass spectrometry to demonstrate differences in H1 variant expression and modification in several mouse organs and also between different cultured cell types.[52] In order to ascertain whether histone H3 variants are expressed or modified differentially in different tissues, we have employed a proteomic approach using a Middle Down mass spectrometry based methodology to systematically characterize the modification patterns of histone H3 variants in a panel of rat tissues. This approach revealed that H3.2 and H3.3 show the greatest differences in expression

and modification between tissues, establishing the basis for future investigations of H3 variant metabolism during cellular differentiation and other processes.

Material and Methods

Histone Extraction and Purification from Selected Rat Tissues

Crude histones were extracted from nuclei prepared from kidney, spleen, brain, bladder, lung, liver, heart, ovary, testes and pancreatic tissue that were cleanly dissected and snap frozen in liquid nitrogen after collection from 7-8 week old Sprague-Dawley rats (Pel-Freez Biologicals, Rogers, AR). Frozen tissues were partially thawed on ice, and we attempted to minimize the effect of differences in tissue structure by removing capsule/connective tissue and mincing tissues into small cubes with razor blades. We then diluted the tissue samples with an excess of nucleus isolation buffer (15 mM Tris-HCl; pH 7.5), 60 mM KCl, 11 mM $CaCl_2$, 5 mM NaCl, 5 mM $MgCl_2$, 250 mM sucrose, 1 mM dithiothreitol, 5 nM microcystin-LR, 500 μM 4-(2-aminoethyl) benzenesulfonyl fluoride (AEBSF), 10 mM sodium butyrate and 0.3% NP-40) before homogenization using a PT 3000 Polytron Homogenizer (Littau, Switzerland). Nuclei were pelleted by centrifugation (500 × g), washed twice with nucleus isolation buffer (without NP-40) and histones extracted with 0.4 N H_2SO_4. Histones were recovered from the extract by 20% trichloroacetic acid (TCA) precipitation followed by washes with acetone/0.1 % HCl and acetone. Crude histone preparations were then dissolved in water and separated by reverse-phase high performance liquid chromatography (RP-HPLC) (System Gold, Beckman Coulter, Fullerton, CA), using a Vydac 208TP54 C8 column (4.6 mm × 250 mm packed with 5 μm diam. particles, 300 angstrom diam. pores; Vydac, Hesperia, CA). Total histones were separated using a gradient of 30-60% solvent B in 100 min. (solvent A = 5% acetonitrile (MeCN) in 0.2% trifluoroacetic acid (TFA) and solvent B = 90% MeCN in 0.188% TFA). RP-HPLC fractions containing histone H3 were dried to dryness to remove organic solvent.

Middle Down Mass Spectrometry Analysis of Histone H3

Histone H3.2 and H3.3 from pooled RP-HPLC fractions were reconstituted in deionized water and digested with endoproteinase Glu-C (Sigma, St. Louis, MO) as previously reported for Middle Down mass spectrometric analysis.[47,48] Briefly, H3 samples were diluted with 100 μL of 100 mM ammonium acetate buffer (pH 4), and incubated with the Glu-C protease at a substrate:enzyme weight ratio of 15:1 for 6 hours at room temperature. The reaction was quenched by freezing at -80°C. The N-terminal fragment (residues 1-50) produced by Glu-C proteolysis was then purified from other digestion products by RP-HPLC as stated above except that a linear gradient of 1% solvent B per minute gradient was used. The RP-HPLC fractions corresponding to the H3.2(1-50) or H3.3(1-50) fragments were pooled and dried to completion.

The H3.2(1-50) or H3.3(1-50) fragments were then diluted with water and methanol (1:1) and 1% formic acid for mass spectrometry analysis. Mass spectrometry data were acquired on a home-built 8.5 Tesla quadrupole-FTMS in positive ion mode using a NanoMate 100 (Advion BioSciences, Ithaca, NY) to introduce the sample into the gas phase via nano-electrospray. We used low flow chips that required <3 μL of solution to automatically establish the spray. The capillary was heated by applying 4 A, and the voltage was set at 2160 V. Charge states of interest (typically 8+ or 9+ charge states) were selectively accumulated using the instrument's quadrupole (ABB Extrel, Houston, TX) with the selection window set at ~ 25 *m/z* centered around the most abundant modified peak and further isolated using Stored Waveform Inverse Fourier Transform (SWIFT).[53] Electron capture dissociation (ECD) with a filament bias of approximately 9V, using 25-200 loops of individual irradiation times of 3 ms and a 10-ms relaxation time between cycles was employed to acquire MS/MS spectra of the histone H3 1-50 polypeptide. Data was collected using the ICR data acquisition system (MIDAS), and fragment ion data collected were analyzed using THRASH and/or manually interpreted.[54]

M_r values of the 1-50 H3 polypeptide and ECD fragment ions are reported for the neutral monoisotopic species. As shown previously by our research group, the ECD MS/MS intensity values of the fragment ion pairs (fragment ion relative ratios, FIRRs) can be utilized to determine the isomeric composition of the precursor ion with an error less than 5% for species producing at least moderate signals.[43,46] In brief, for calculating FIRR values for histone H3 we measured the ECD fragment intensity (typically of the first two monoisotopic peaks) corresponding to the different modified forms of the same residue (i.e. for the unmodified, mono-, di-, and trimethylated signals from the K9 residue, c_9^{2+} ions at 529, 536, 543 and 550 *m/z* were measured) and expressed each as the ratio of that modified form to the total intensity of all of the modified forms of that residue. Therefore for histone H3 monomethylation, we expressed this modification as the ratio of the 536 *m/z* ion over the sum of the 529, 536, 543 and 550 *m/z* ions. Ions used for FIRR calculation include the c_4^+ ion for the K4 residue, the c_9^{2+} ion for the K9 residue, the c_{24}^{3+} ion for the K23 residue, the $z\cdot_{24}^{3+}$ or $z\cdot_{27}^{3+}$ ion for the K27 residue and the $z\cdot_{15}^{3+}$ ion for the K36 residue.

Results and Discussion

H3 Variant Expression in Different Rat Tissues

We compared the expression and posttranslational modifications of histone H3 variants in ten selected rat organs. Total histones were acid extracted from nuclei isolated from the following rat organs: brain, liver, lung, bladder, heart, ovary, spleen, pancreas, testes and kidney. Histone H3 variants were resolved and separated from the other histones using RP-HPLC as previously described.[43] RP-HPLC chromatograms displaying the separation of total histones from nine of these organs are shown in Figure 1 with the major peaks identified by mass spectrometry (data not shown) labeled in the chromatogram for the bladder histones (Fig. 1A). Histone H2B typically elutes first followed by a peak containing H2A, then H4, followed another peak containing H2A proteins. The difference in elution times for H2A stems from the oxidation of the H2A proteins in the first peak as previously noted.[44] Lastly, three peaks corresponding to the histone variant family members H3.2, H3.3 and H3.1 elute several minutes later. This elution order is very similar to that demonstrated previously for histones extracted from cultured mammalian cell lines such as HeLa or HEK.[43,55,56] H3.2 was the most abundant variant in all tissues examined except for testes. The abundance of H3.3 approached that of H3.2 in such as brain, testes and heart, but H3.2 was 2-3 times more abundant than H3.3 in most cases. Variation in H3.3 expression may prove to be significant, as this histone H3 variant has been reported to be preferentially associated with transcriptionally active gene loci[57] and has been reported to be covalently modified with PTMs associated with gene activation.[56, 58-60] Additionally, H3.3 is also incorporated into chromatin in a replication independent manner in contrast to H3.2 which is deposited during DNA replication.[57,61] In general, H3.1 was the least abundant variant in most tissues but was present in an amount similar to H3.3 in spleen (Fig. 1C) and was the major form of H3 present in testes (Fig. 1I). These relative abundances differ from those described previously for several cultured mammalian cell lines.[43,55,56] Because H3.2 and H3.3 were the most abundant variants in nearly all the rat tissues, and because the sequences of these two variants are conserved in many organisms (H3.1 is present only in mammalian species),[62] we decided to investigate their PTM profiles using our Middle Down mass spectrometry platform.

Interrogation of H3 PTM Profiles by Middle Down Mass Spectrometry

After purifying the H3.2 and H3.3 variants, we digested them with GluC, which cleaves the proteins into several peptides, including the fragment spanning residues 1-50 that contains the majority of the PTMs known to occur on these proteins.[2] The 1-50 fragment was separated from the other digestion products by RP-HPLC. We then obtained mass spectra of RP-HPLC purified histone H3.2(1-50) and H3.3(1-50) polypeptides prepared from each of the tissues and

using the high mass accuracy of the FTMS, we assigned preliminary modification states to the peaks observed and detected potential differences in modification between the samples. Figure 2 displays the broadband mass spectra from nine of the ten tissue types. Figure 2A shows the mass spectrum of H3.2(1-50) from a bladder sample, and the first major peak observed had a mass of 5394.18 Da. Comparison to the theoretical mass of H3.2(1-50) (5338.07 Da) suggested that the Δ*m* was ~56 Da or the addition of four methyl group equivalents. The calculated mass of H3.2(1-50) with the addition of four methyl groups is 5394.13 Da, very close to the observed mass. More peaks in the spectrum differing by the addition of 14 Da can be seen, and H3.2 (1-50) containing 4-12 methyl group equivalents were easily detectable for most tissues with the apex peaks corresponding to 6 or 7 methyl group equivalents. However, H3.2(1-50) from liver, heart and testes (Fig. 2D, E and I) appeared to be hypomodified in comparison to the other rat tissues. These three tissue types had methyl group distributions ranging from 4 to only 9 methyl groups with the apex peak containing 5 or 6 methyl group equivalents. Unexpectedly, we found that these tissue differences in bulk modification were also characteristic of the histone H3.3 variant (Supplemental Figure 1), in that H3.3(1-50) isolated from liver, heart and testes appeared to be less modified than in other tissues.

Localization and Relative Quantification of PTMs on Histone H3 by ECD

Our analyses of H3.2(1-50) and H3.3(1-50) from various rat organs demonstrated apparent differences in PTM levels between tissues (especially liver, heart and testes), so we sought to characterize and localize the modification sites on the H3 proteins using MS/MS experiments on the FTMS. For our tandem mass spectrometry studies, we used a multiplexed ECD procedure that we demonstrated previously is effective for analyses of H3 acetylation and methylation, in which all forms are fragmented *en masse*.[43] Figure 3 displays our ECD-based approach for the characterization of PTM sites on histone H3.2(1-50) prepared from kidney tissue. As shown in Figure 3A, the most prominent charge states observed in the broadband mass spectrum were the 10+, 9+ and 8+ charge states. Using the 8+ charge state as an example, we performed a quadrupole enhancement of this charge state and further filtered the *m/z* species by SWIFT to fully isolate this charge state from the others (as shown in the Figure 3A inset). ECD was then performed (Figure 3B) on all the differently modified forms of H3.2(1-50) within the selected charge state. Careful inspection of the fragment ions revealed site specific information, as shown for the c_9^{2+} ions corresponding to modifications at un, mono-, di-, and trimethylation at K9 (528-552 *m/z*) and the $z\cdot_{15}^{2+}$ ions corresponding to un, mono- and dimethylation at K36 (894-912 *m/z*). The resolving power and highly accurate mass of FTMS allows distinction between fragment ions harboring trimethylation versus acetylation marks (Δ*m* = 0.036 Da). In this case, the observed c_9^{2+} ion at 1099.70 Da is consistent with trimethylation (calculated = 1099.69 Da) and not acetylation (calculated = 1099.66 Da). Fragment ions can be searched using the ProSight software or manually validated to create a graphical fragment map (Figure 3C). Since all forms of histone H3.2 are fragmented in parallel in this multiplex ECD procedure, the fragment map displays the aggregate distribution of modifications on the particular H3 variant analyzed. We determined that the most abundant modifications in this sample of bulk kidney H3.2 were K9me2, K23ac, K27me2 and K36me2 (fragment map in Figure 3C).

Using this Middle Down approach we interrogated the PTM status on RP-HPLC purified H3.2 (1-50) and H3.3(1-50) polypeptides prepared from the ten selected rat tissues and determined that the most abundant modifications in general were: monomethylation on lysine 4 (K4me1), mono-, di- and trimethylation on lysine 9 (K9me1, K9me2 and K9me3), acetylation on lysine 23 (K23ac), mono-, di- and trimethylation on lysine 27 (K27me1, K27me2 and K27me3) and mono- and dimethylation on lysine 36 (K36me1 and K36me2). However, specific differences in the abundance of certain H3.2 PTMs were consistently observed between different tissue types when the results for three independent preparations from each tissue were compared. For

example in Figure 4, we show an ECD mass spectrum focusing on the *m/z* region that reports the c_9^{2+} fragment ions (modifications on the K9 residue) from bladder (Fig. 4A) and testes (Fig. 4B) tissue samples. As is clearly seen, the relative abundance of the different K9 methylation states differs in H3.2(1-50) prepared from these tissues. In bladder tissue, K9me2 is the most abundant modification followed by K9me3 > unmodified K9 > K9me1. In contrast, K9me3 is the most abundant modification followed by unmodified K9 > K9me2 > K9me1 in testes. Using the FIRRs from the ECD spectra, we can relatively quantify the levels of modification at sites in histone H3, as described in Materials and Methods, and as shown previously for quantification of differently modified isomeric forms of histone H3 and H4.[43,46,63] A histogram showing the distribution of K9 methylation on H3.2(1-50) from the various tissues is displayed in Figure 5A, while the K9 methylation distribution on H3.3(1-50) is shown in Figure 5B. Dimethylation was the most abundant methylation mark on the K9 residue of H3.2(1-50) in all tissues except testes (Fig. 5A). However, the ratios of the different degrees of methylation varied slightly among different tissues. For example, in H3.2(1-50) from heart, lung and ovary tissue, K9me2 and K9me3 were found in a nearly 1:1 ratio, whereas in most other tissues K9me2 was significantly more abundant than K9me3. In H3.2(1-50) from testes, K9me3 was more abundant than either of the lower methylated states. Similarly, differences in the modification of K9 in the H3.3 variant between tissues were also evident as shown by inspection of ECD spectra taken of histone H3.3(1-50) from lung (Figure 6A) and spleen (Figure 6B). Zoom regions containing c_9^{2+} and $z^{\cdot}{}_{15}^{2+}$ fragment ions (528-552 and 894-912 *m/z*, respectively) show that slight differences in lung and spleen occur in K9 methylation, and even larger differences are seen in K36 methylation (larger amount of unmodified K36). The histograms in Figure 5B show the variation in K9 methylation of H3.3 (1-50) among the tissues analyzed. Apart from testes and spleen, we found that K9me2 was the most abundant form present in H3.3 from most tissues, as noted for H3.2 (compare Figures 5A and 5B). However, in many cases, significant differences in the relative abundance of each K9 methylation state were observed between H3.2 and H3.3 within the same tissue that are consistent with the notion that these variants are functionally distinct.

Using the ECD spectra of the H3.2(1-50) and H3.3(-50) polypeptides from different tissues, we then characterized the modifications present at K4, K23, K27 and K36, the remaining abundantly modified sites in the H3.2 and H3.3 variants. Supplemental Figures 2-5 display histograms depicting the PTM distributions on these lysines in the H3.2(1-50) and H3.3(1-50) polypeptides prepared from our set of tissues. As shown in Supplemental Figure 2, K4 was largely unmodified on both H3.2 and H3.3 in all tissues examined with relatively low levels of monomethylation detectable in each case. From prior estimates,[48] the Middle Down approach as implemented here can detect histone forms present in greater than ~500,000 nucleosomes. However, many of the lower abundance marks detectable by antibodies and important in epigenetic regulation (e.g. H3K4me3) are not detectable by the current approach. K4me2 and K4me3 have been detected in many cell types using immunochemical methods, nevertheless, our results suggest that these modifications must be present at levels less than a few percent as they are below our proteomic detection limit.[48,63] On average, monomethylation affected approximately 5% of H3.2 in most tissues (ovary tissue was the exception with approximately 15 % of H3.2 containing K4me1). In contrast, the levels of K4me1 were approx. 3 fold higher in H3.3 from most tissue types (average closer to 15%). This difference is readily evident when the ECD spectra of H3.2(1-50) and H3.3(1-50) from heart tissue are compared as shown in Figure 7. The finding that K4me1 levels are higher in H3.3 compared to H3.2 in a wide variety of tissues, combined with the evidence that H3.3 is preferentially enriched in transcriptionally active chromatin,[56,58-60] supports the notion the K4 methylation in general (i.e. me1, me2 and me3) functions in transcriptional regulation.

Supplemental Figure 4 displays the variation in K23ac in the various tissues for both H3 variants. Hypoacetylation at this residue was observed in both H3.2(1-50) and H3.3(1-50) from

the heart, liver and testes samples. The relative abundance of K23 acetylation was very similar for H3.2(1-50) and H3.3(1-50) from almost all tissues, in contrast to the increased abundance of K4me1 in H3.3 compared to H3.2 noted above. It is curious to note that we detect only a modest amount of acetylation which occurs predominantly at K23. Whether lower acetylation levels are typical of tissues compared to cultured cells remains unresolved, but recently a publication has suggested differences in histone H1 modification exist between cultured mouse cells and tissues.[52] The greatest differences in relative PTM abundance between H3.2 and H3.3 in different tissues were observed for methylations at K27. These were monitored by detecting ECD fragments corresponding to $z^{\cdot}_{24}{}^{3+}$ or $z^{\cdot}_{24}{}^{3+}$ ions and histograms summarizing the degree of methylation (mono-, di- and trimethylation) on this residuefrom H3.2(1-50) and H3.3(1-50) from the different tissues are shown in Supplemental Figure 4. Unmodified K27 predominated in both H3.2 and H3.3 from bladder, heart, liver and testes samples. In contrast, although K27me1 was the predominant form in H3.2 from kidney, lung, ovary, pancreas and spleen, K27me2 predominated in H3.3 from these same tissues. In general, the levels of K27me3 were higher in H3.2 compared to H3.3 from the same tissue: an extreme example of this occurred in brain where the level of K27me3 in H3.2 (approx. 42 %) was three-fold higher than that in H3.3 (approx. 14 %). The large variations we observed in K27 methylation degree between H3.2 and H3.3 in different tissues suggest that methylation at this site may play a role in developmentally regulated changes in gene expression that occur during differentiation and which ultimately lead to the formation of specific tissues. Supporting this notion is the recent finding that the methyltransferase responsible for K27 methylation in mammals (Ezh2) has been reported to regulate skeletal muscle differentiation by promoting muscle gene expression[21] and has been shown to regulate expression of developmental genes in embryonic stem cell differentiation.[20,22,23]

Finally, the modification status of K36 in H3.2(1-50) and H3.3(1-50) from the various tissues is shown in Supplemental Figure 5. To date, K36 methylation is the only histone modification reported to be enriched at the 3′ end of active genes,[64] but little is known about whether functional differences exist between mono-, di- and trimethylation at this site. Although H3K36me3 has been demonstrated in human/metazoan samples previously by immunochemical approaches, we did not detect it here or in previous analyses which utilized two dimensional chromatography to enrich less abundant forms of HeLa cell H3.2 prior to mass spectrometry.[48] Thus, we infer that molecules bearing this modification probably represent less than 2 % of total histone H3.[63] We found that the levels of unmodified K36, or K36me1, or K36me2 in H3.2 varied substantially between tissues with some (heart, liver, lung, pancreas, spleen, testes) containing predominantly unmodified K36, while others (kidney, ovary) contained predominantly K36me2, or contained both forms in similar amounts (bladder, brain) (Supplemental Figure 5A). Strikingly, K36me2 was the overwhelmingly predominant form of H3.3 observed for all tissues except testes (Supplemental Figure 5B). Comparing the results for K36 methylation between H3.2(1-50) and H3.3(1-50) from various tissues, it becomes apparent that while unmodified K36 predominates in H3.2 in most tissues, K36 is preferentially dimethylated in H3.3 in these same tissues.

Overall, these results show that the global levels of H3 modifications differ in different tissues, suggesting that these differences in abundance reflect the roles of these PTMs in epigenetic mechanisms contributing to differential gene expression in these tissues. Our results correlate well with another proteomic study of lysine methylation and acetylation in mouse[65] Using anti-methyllysine and anti-acetyllysine antibodies, Iwabata et al. showed that a organs. variety of proteins including histones were variably modified by lysine methylation and acetylation in different selected mouse organs. The authors also discovered that H3 and H4 were both globally underacetylated and undermethylated in heart, stomach, kidney, skeletal muscle and liver but were hypermodified with those same marks in lung, spleen, brain, small intestine and colon tissue.

Identification of a Novel Rat Testes-Specific H3 variant

A strong advantage in using mass spectrometry for analysis of histone PTMs as opposed to antibody based methods is the ability to discover novel PTM sites or identify histone variant family members. Here we report the identification of a new histone H3 variant that was detected only in testes samples. During the RP-HPLC purification of histone H3 variants (Fig. 1), we noticed that expression of the H3.1 variant was lower than the H3.2 or H3.3 variants in all tissues except testes. In testes samples, a peak eluting at the same time point normally observed for H3.1 was the predominant form and we initially assumed that this peak contained only H3.1. However, in the course of attempting to analyze modifications on the 1-50 Glu-C fragment generated from this fraction, we found that the mass of the 1-50 fragment (5375.10 Da), did not match the unmodified or potentially modified masses for the corresponding fragments of the canonical rat H3.1, H3.2 and H3.3 protein sequences. As shown in the broadband mass spectrum of the +8 charge state of this 1-50 polypeptide (Figure 8A), a few peaks separated by 14 Da are evident suggesting that the protein is modified. We obtained an ECD spectrum (Fig. 8B) of the unknown species and identified several *c*-type ions which suggested that this protein was similar to histone H3. Nevertheless, aside from a few $z\cdot$-type ions at the extreme C-terminus, we did not $z\cdot$-type ions that matched the fragmentation spectrum to the sequences for established find many rat H3 family members. However, a search of the NCBI database for rat H3-like proteins sequences revealed an entry ‘predicted: similar to H3 histone family member’ (accession # XP_220509) that fit the ECD fragmentation pattern. This novel H3 protein, which we call rat H3.1T, has two amino acid substitutions within the first 50 residues when compared to the rat H3.2 or H3.1 sequences (Figure 8C), an A → V change at position 24, and an R → H change at position 42. The mass of the $z\cdot_9^+$ ion at 962.503 Da shown in the zoom region in the ECD spectrum in Figure 8B is consistent with the R → H change on this protein (calculated mass of the $z\cdot_9^+$ ion is 962.506 Da). The experimental mass of the first species of the H3.1T(1-50) polypeptide observed in the broadband mass spectrum in Figure 8A was 5375.10 Da which fits very well with the calculated mass of a dimethylated form of the H3.1T(1-50) polyprotein (5375.09 Da). In addition, we acquired the mass of intact H3.1T (15,316.5 Da), and found that to be in agreement with the calculated dimethylated form of the intact protein at 15,316.4 Da (data not shown). We did not observe expression of the standard H3.1 protein in testes, nor did we observe expression of this particular H3.1T in other tissues (data not shown), further supporting the notion that this variant may fulfill a testes-specific function. Testes-specific H3 variants have been uncovered in human and mouse, and we now can add rat to the list of mammals expressing a testes-specific H3 protein. Lastly, the ECD data (Figure 8C) show that this variant is similar to other H3 variants from testes and is hypomodified at many residues. This mass spectrometry data supports the finding of a novel rat testes-specific variant H3.1T whose biological significance remains to be determined.

Conclusion

Histone posttranslational modifications (PTMs) have been shown to be important regulators of gene expression during critical developmental periods such as tissue formation, and this characteristic PTM pattern is likely to be inherited epigenetically and distinct among various organs or tissue types. Using a Middle Down proteomics platform, we have interrogated the PTM profiles of histone H3 variants from ten selected rat organs: bladder, brain, heart, kidney, liver, lung, ovary, pancreas, spleen and testes. RP-HPLC revealed slight differences in the relative expression of H3 variants between these tissues, with the largest differences observed in testes. Electron capture dissociation (ECD) fragmentation was utilized to obtain tandem mass spectra for localization of the modified residues on the H3 variants, and the FIRRs were applied to relatively quantify the site occupancy of the most abundantly modified H3 residues: K4, K9, K23, K27 and K36. This comparison of H3 PTMs from different tissues showed that differences in global abundance of PTMs exist among the different tissue types. For example,

histone H3 extracted from heart, liver and testes tissue were distinguishably undermodified, albeit at different residues and to differing degrees. Lastly, we report the identification of a novel rat histone H3 protein that is highly expressed in testes and that was previously cataloged in protein databases as a 'predicted, similar to histone H3 family member' protein. These data demonstrate the feasibility of Middle Down mass spectrometry for quantification of PTM sites and abundance levels, and for discovery of novel protein isoforms from mammalian tissues. Changes in histone modification and chromatin structure are increasingly being shown to be important for the development of multicellular organisms. We suggest that the methodology employed here will prove useful in future studies regarding epigenetic control of cellular differentiation and/or tissue formation.

Supplementary Material

Refer to Web version on PubMed Central for supplementary material.

Acknowledgments

We are grateful for funding from the NIH (GM 067193), the Alfred P. Sloan Foundation, the Packard Foundation and a 2004 Camille Dreyfus Teacher-Scholar Award from the Dreyfus Foundation to N.L.K. C.A.M. acknowledges support from the Roy J. Carver Charitable Trust (grant 04-76) and the March of Dimes (Basil O'Connor Scholar Award 5-FY05-1232). B.A.G. is supported by the Institute of Genomic Biology at the University of Illinois and an NIH NRSA fellowship (1 F32 GM 078942-01).

References

1. Luger K, Mader AW, Richmond RK, Sergeant DF, Richmond TJ. Nature 1997;389:251–260. [PubMed: 9305837]
2. Turner BM. Nat. Struct. Mol. Biol 2005;12:110–112. [PubMed: 15702071]
3. Lachner M, O'Carroll D, Rea S, Mechtler K, Jenuwein T. Nature 2001;410:116–120. [PubMed: 11242053]
4. Santos-Rosa H, Schneider R, Bannister AJ, Sherriff J, Bernstein BE, Emre NC, Schreiber SL, Mellor J, Kouzarides T. Nature 2002;419:407–411. [PubMed: 12353038]
5. van Leeuwen F, Gafken PR, Gottschling DE. Cell 2002;109:745–756. [PubMed: 12086673]
6. Bannister AJ, Schneider R, Myers FA, Thorne AW, Crane-Robinson C, Kouzarides T. J. Biol. Chem 2005;280:17732–17736. [PubMed: 15760899]
7. Vidanes GM, Bonilla CY, Toczyski DP. Cell 2005;121:973–976. [PubMed: 15989948]
8. Kouzarides T. Cell 2007;128:693–705. [PubMed: 17320507]
9. Polioudaki H, Markaki Y, Kourmouli N, Dialynas G, Theodoropoulos PA, Singh PB, Georgatos SD. FEBS Lett 2004;560:39–44. [PubMed: 14987995]
10. Wei Y, Mizzen CA, Cook RG, Gorovsky MA, Allis CD. Proc. Natl. Acad. Sci. U S A 1998;95:7480–7484. [PubMed: 9636175]
11. Goto H, Tomono Y, Ajiro K, Kosako H, Fujita M, Sakurai M, Okawa K, Iwamatsu A, Okigaki T, Takahashi T, Inagaki M. J. Biol. Chem 1999;274:25543–25549. [PubMed: 10464286]
12. Son CG, Bilke S, Davis S, Greer BT, Wei JS, Whiteford CC, Chen QR, Cenacchi N, Khan J. Genome Res 2005;15:443–450. [PubMed: 15741514]
13. Shyamsundar R, Kim YH, Higgins JP, Montgomery K, Jorden M, Sethuraman A, van de Rijn M, Botstein D, Brown PO, Pollack JR. Genome Biology 2005;6:R22. [PubMed: 15774023]
14. Liang S, Li Y, Be X, Howes S, Liu W. Physiol. Genomics 2006;26:158–162. [PubMed: 16684803]
15. Jones PA, Martienssen R. Cancer Res 2005;65:11241–11246. [PubMed: 16357125]
16. Callinan PA, Feinberg AP. Hum. Mol. Genet 2006;15:R95–101. [PubMed: 16651376]
17. Lee JH, Hart SR, Skalnik DG. Genesis 2004;38:32–38. [PubMed: 14755802]
18. Szutorisz H, Canzonetta C, Georgiou A, Chow CM, Tora L, Dillon N. Mol Cell Biol 2005;25:1804–1820. [PubMed: 15713636]

19. Margueron R, Trojer P, Reinberg D. Curr. Opin. Genet. Dev 2005;15:163–176. [PubMed: 15797199]
20. Boyer LA, Plath K, Zeitlinger J, Brambrink T, Medeiros LA, Lee TI, Levine SS, Wernig M, Tajonar A, Ray MK, Bell GW, Otte AP, Vidal M, Gifford DK, Young RA, Jaenisch R. Nature 2006;441:349–353. [PubMed: 16625203]
21. Caretti G, Di Padova M, Micales B, Lyons GE, Sartorelli V. Genes Dev 2004;18:2627–2638. [PubMed: 15520282]
22. Bernstein BE, Mikkelsen TS, Xie X, Kamal M, Huebert DJ, Cuff J, Fry B, Meissner A, Wernig M, Plath K, Jaenisch R, Wagschal A, Feil R, Schreiber SL, Lander E,S. Cell 2006;125:315–326. [PubMed: 16630819]
23. Agger K, Cloos PA, Christensen J, Pasini D, Rose S, Rappsilber J, Issaeva I, Canaani E, Salcini AE, Helin K. Nature 2007;449:731–734. [PubMed: 17713478]
24. Strahl BD, Briggs SD, Brame CJ, Caldwell JA, Koh SS, Ma H, Cook RG, Shabanowitz J, Hunt DF, Stallcup MR, Allis CD. Curr. Biol 2001;11:996–1000. [PubMed: 11448779]
25. Banks GC, Deterding LJ, Tomer KB, Archer TK. J. Biol. Chem 2001;276:36467–36473. [PubMed: 11479299]
26. Zhang K, Tang H, Huang L, Blankenship JW, Jones PR, Xiang F, Yau PM, Burlingame AL. Anal. Biochem 2002;306:259–269. [PubMed: 12123664]
27. Galasinski SC, Louie DF, Gloor KK, Resing KA, Ahn NG. J. Biol. Chem 2002;277:2579–2588. [PubMed: 11709551]
28. Freitas MA, Sklenar AR, Parthun MR. J. Cell Biochem 2004;92:691–700. [PubMed: 15211567]
29. Garcia BA, Busby SA, Barber CM, Shabanowitz J, Allis CD, Hunt DF. J. Proteome Res 2004;3:1219–1227. [PubMed: 15595731]
30. Bonaldi T, Imhof A, Regula JT. Proteomics 2004;4:1382–1396. [PubMed: 15188406]
31. Burlingame AL, Zhang X, Chalkley RJ. Methods 2005;36:383–394. [PubMed: 16112065]
32. Garcia BA, Barber CM, Hake SB, Ptak C, Turner FB, Busby SA, Shabanowitz J, Moran RG, Allis CD, Hunt DF. Biochemistry 2005;44:13202–13213. [PubMed: 16185088]
33. Chu F, Nusinow DA, Chalkley RJ, Plath K, Panning B, Burlingame AL. Mol.Cell. Proteomics 2006;5:194–203. [PubMed: 16210244]
34. Bonenfant D, Coulot M, Towbin H, Schindler P, van Oostrum J. Mol Cell Proteomics 2006;5:541–552. [PubMed: 16319397]
35. Ouvry-Patat SA, Schey KL. J. Mass Spectrom 2007;42:664–674. [PubMed: 17405180]
36. Chen Y, Sprung R, Tang Y, Ball H, Sangras B, Kim SC, Falck JR, Peng J, Gu W, Zhao Y. Mol. Cell. Proteomics 2007;6:812–819. [PubMed: 17267393]
37. Jiang T, Zhou X, Taghizadeh K, Dong M, Dedon PC. Proc. Natl. Acad. Sci. U S A 2007;104:60–65. [PubMed: 17190813]
38. Garcia BA, Joshi S, Thomas CE, Chitta RK, Diaz RL, Busby SA, Andrews PC, Ogorzalek Loo RR, Shabanowitz J, Kelleher NL, Mizzen CA, Allis CD, Hunt DF. Mol Cell Proteomics 2006;5:1593–609. [PubMed: 16835217]
39. Beck HC, Nielsen EC, Matthiesen R, Jensen LH, Sehested M, Finn P, Grauslund M, Hansen AM, Jensen ON. Mol Cell Proteomics 2006;5:1314–1325. [PubMed: 16627869]
40. Garcia BA, Busby SA, Shabanowitz J, Hunt DF, Mishra N. J Proteome Res 2005;4:2032–2042. [PubMed: 16335948]
41. Pesavento JJ, Kim YB, Taylor GK, Kelleher NL. J. Am. Chem. Soc 2004;126:3386–3387. [PubMed: 15025441]
42. Medzihradszky KF, Zhang X, Chalkley RJ, Guan S, McFarland MA, Chalmers MJ, Marshall AG, Diaz RL, Allis CD, Burlingame AL. Mol. Cell Proteomics 2004;3:872–886. [PubMed: 15199121]
42. Zhang L, Freitas MA. Int. J. Mass Spectrom 2004;234:213–225.
43. Thomas CE, Kelleher NL, Mizzen CA. J. Proteome Res 2006;5:240–247. [PubMed: 16457588]
44. Boyne MT 2nd, Pesavento JJ, Mizzen CA, Kelleher NL. J. Proteome Res 2006;5:248–253. [PubMed: 16457589]
45. Siuti N, Roth MJ, Mizzen CA, Kelleher NL, Pesavento JJ. J. Proteome Res 2006;5:233–239. [PubMed: 16457587]

46. Pesavento JJ, Mizzen CA, Kelleher NL. Anal. Chem 2006;78:4271–4280. [PubMed: 16808433]
47. Taverna SD, Ueberheide BM, Liu Y, Tackett AJ, Diaz RL, Shabanowitz J, Chait BT, Hunt DF, Allis CD. Proc. Natl. Acad. Sci. U S A 2007;104:2086–2091. [PubMed: 17284592]
48. Garcia BA, Pesavento JJ, Mizzen CA, Kelleher NL. Nat. Methods 2007;4:487–489. [PubMed: 17529979]
49. Lindroth AM, Shultis D, Jasencakova Z, Fuchs J, Johnson L, Schubert D, Patnaik D, Pradhan S, Goodrich J, Schubert I, Jenuwein T, Khorasanizadeh S, Jacobsen SE. EMBO J 2004;23:4286–4296. [PubMed: 15457214]
50. Fischle W, Tseng BS, Dormann HL, Ueberheide BM, Garcia BA, Shabanowitz J, Hunt DF, Funabiki H, Allis CD. Nature 2005;438:1116–1122. [PubMed: 16222246]
51. Taverna SD, Ilin S, Rogers RS, Tanny JC, Lavender H, Li H, Baker L, Boyle J, Blair LP, Chait BT, Patel DJ, Aitchison JD, Tackett AJ, Allis CD. Mol Cell 2006;24:785–796. [PubMed: 17157260]
52. Wisniewski JR, Zougman A, Kruger S, Mann M. Mol. Cell Proteomics 2007;6:72–87. [PubMed: 17043054]
53. Patrie SM, Charlebois JP, Whipple D, Kelleher NL, Hendrickson CL, Quinn JP, Marshall AG, Mukhopadhyay B. J. Am. Soc. Mass Spectrom 2004;15:1099–1108. [PubMed: 15234368]
54. Senko MW, Hendrickson CL, Pasa-Tolic L, Marto JA, White FM, Guan S, Marshall AG. Rapid Commun. Mass Spectrom 1996;10:1824–1828. [PubMed: 8953784]
55. Hake SB, Garcia BA, Kauer M, Baker SP, Shabanowitz J, Hunt DF, Allis CD. Proc Natl Acad Sci U S A 2005;102:6344–6349. [PubMed: 15851689]
56. Hake SB, Garcia BA, Duncan EM, Kauer M, Dellaire G, Shabanowitz J, Bazett-Jones DP, Allis CD, Hunt DF. J. Biol. Chem 2006;281:559–568. [PubMed: 16267050]
57. Ahmad K, Henikoff S. Mol. Cell 2002;9:1191–1200. [PubMed: 12086617]
58. McKittrick E, Gafken PR, Ahmad K, Henikoff S. Proc Natl Acad Sci U S A 2004;101:1525–1530. [PubMed: 14732680]
59. Loyola A, Bonaldi T, Roche D, Imhof A, Almouzni G. Mol Cell 2006;24:309–316. [PubMed: 17052464]
60. Garcia BA, Siuti N, Thomas CE, Mizzen CA, Kelleher NL. Int. J. Mass Spectrom 2007;259:184–196.
61. Jin J, Cai Y, Li B, Conaway RC, Workman JL, Conaway JW, Kusch T. Trends Biochem. Sci 2005;30:680–687. [PubMed: 16257529]
62. Hake SB, Allis CD. Proc Natl Acad Sci U S A 2006;103:6428–6435. [PubMed: 16571659]
63. Pesavento JJ, Garcia BA, Streeky JA, Kelleher NL, Mizzen CA. Mol. Cell.Proteomics 2007;6:1510–1526. [PubMed: 17569892]
64. Bannister AJ, Schneider R, Myers FA, Thorne AW, Crane-Robinson C, Kouzarides T. J. Biol. Chem 2005;280:17732–17736. [PubMed: 15760899]
65. Iwabata H, Yoshida M, Komatsu Y. Proteomics 2005;5:4653–4664. [PubMed: 16247734]

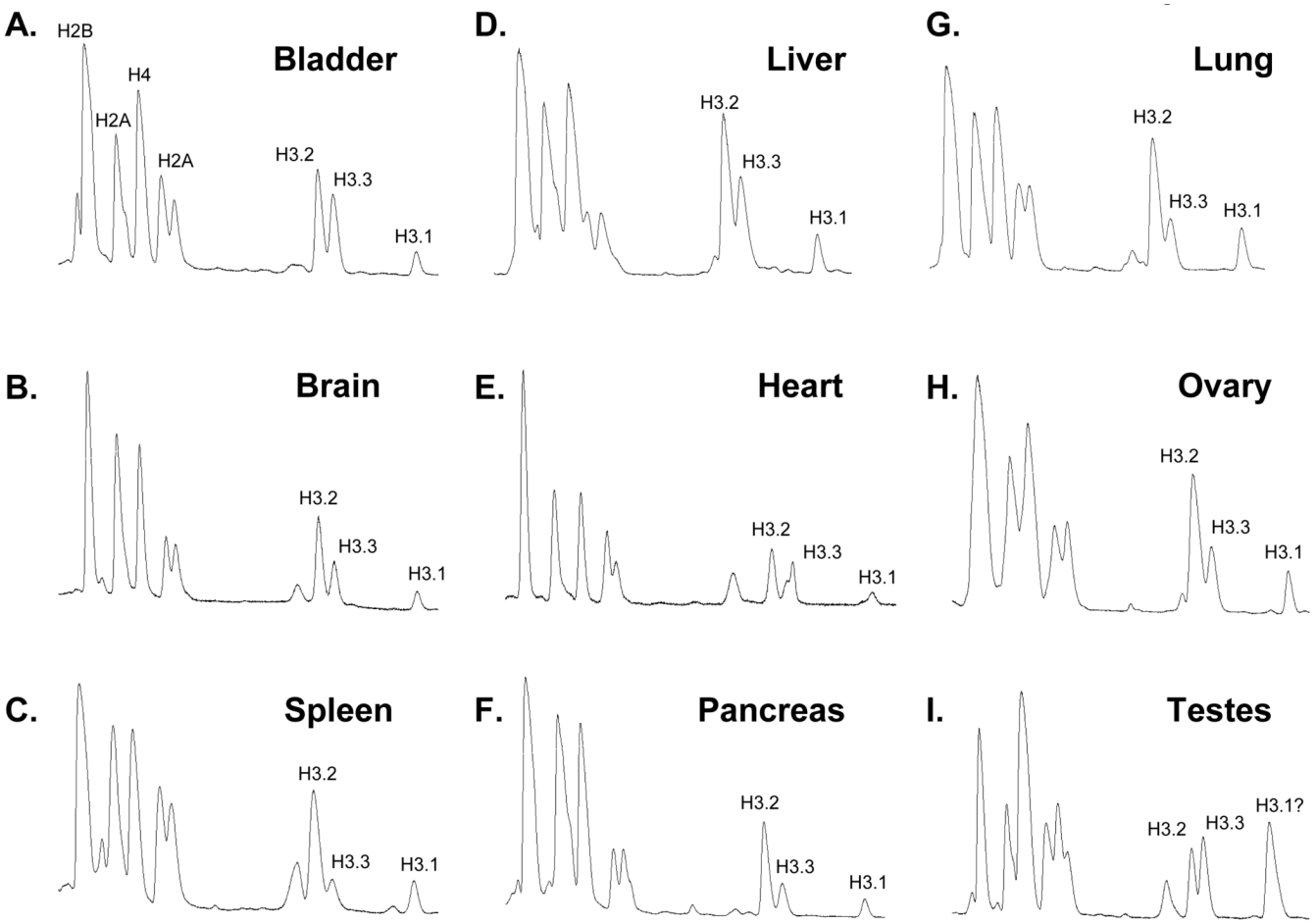

Figure 1.

RP-HPLC chromatograms showing the separation of bulk histones isolated from rat (**A.**) bladder, (**B.**) brain, (**C.**) spleen, (**D.**) liver, (**E.**) heart, (**F.**) pancreas, (**G.**) lung, (**H.**) ovary and (**I.**) testes. Various histone family members are fully labeled in (**A.**) bladder samples, and histone H3 variants are labeled in all chromatograms. The presence of a highly expressed H3.1-like protein in (**I.**) testes was detected.

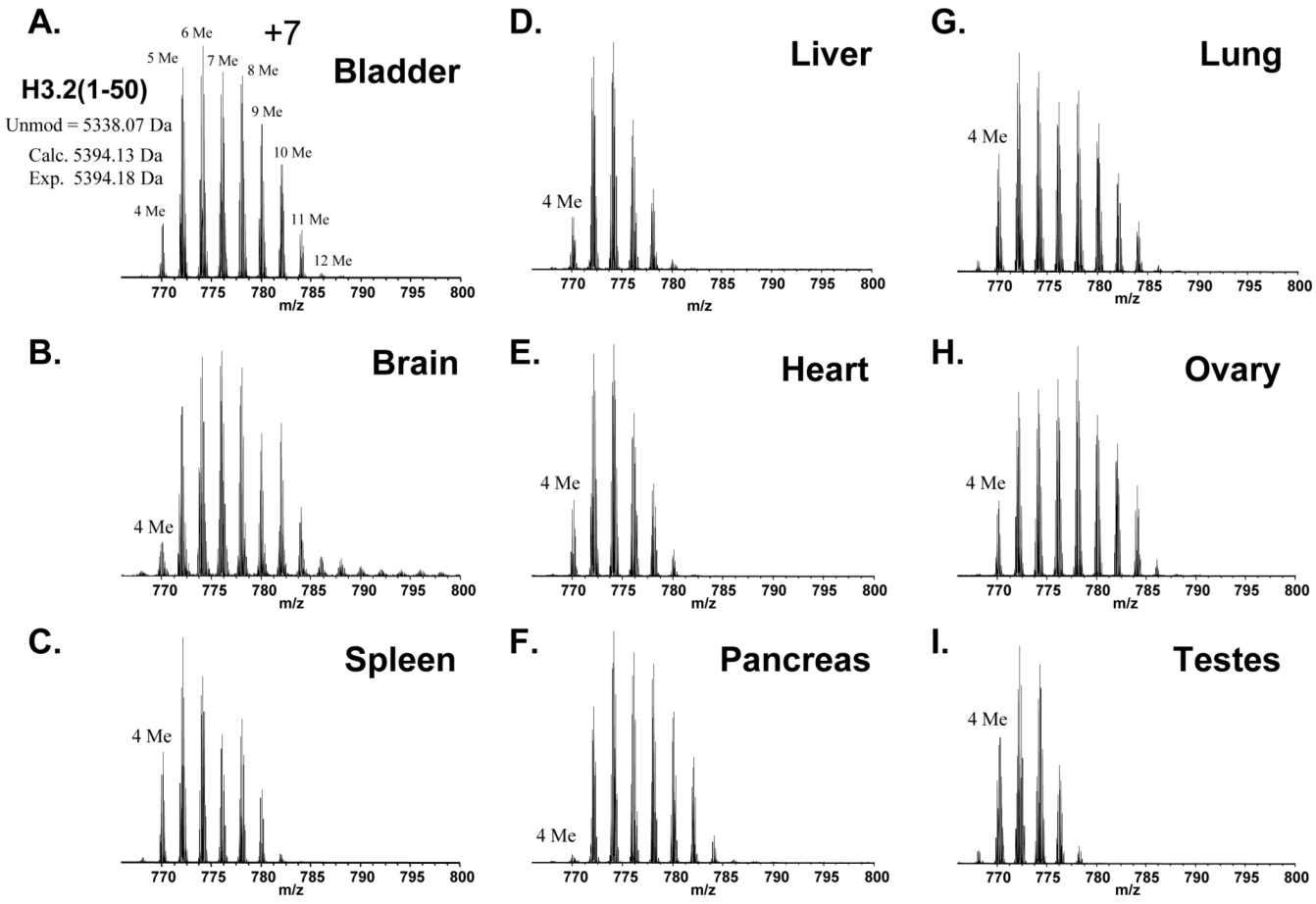

Figure 2.

Broadband mass spectra of the 7+ charge state of the histone H3.2(1-50) polypeptide extracted from rat (**A.**) bladder, (**B.**) brain, (**C.**) spleen, (**D.**) liver, (**E.**) heart, (**F.**) pancreas, (**G.**) lung, (**H.**) ovary and (**I.**) testes. Calculated and experimental mass of the 4 Me species is shown for the bladder sample (A).

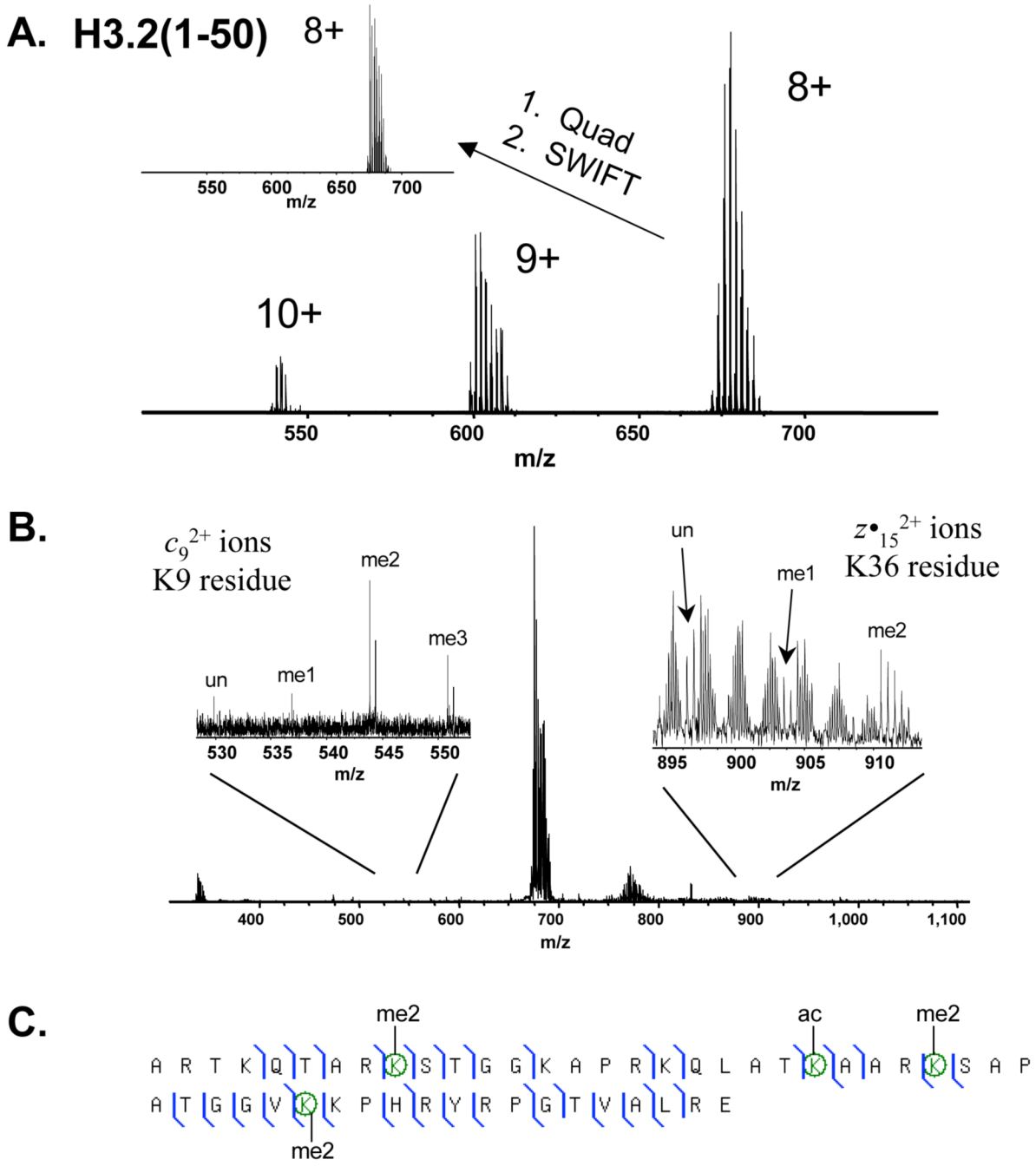

Figure 3.

A. Broadband mass spectrum of the 8+, 9+ and 10+ charge states of the histone H3.2(1-50) polypeptide from rat kidney. Further isolation of the 8+ charge state species is achieved through additional quadrupole enhancement and SWIFT isolation as shown in the inset mass spectrum. **B.** ECD fragmentation of the 8+ charge state species isolated in (**A.**). Zoom regions spanning 528-552 *m/z* and 895-912 *m/z* show regions containing fragment ions which correspond to posttranslational modifications on K9 (unmodified, mono-, di- and trimethylation) and K36 (unmodified, mono- and dimethylation), respectively. **C.** ECD fragment map generated from the fragmentation spectrum shown in (**B.**). Some of the most common modifications observed on histone H3.2 from rat kidney are K9me2K23acK27me2K36me2.

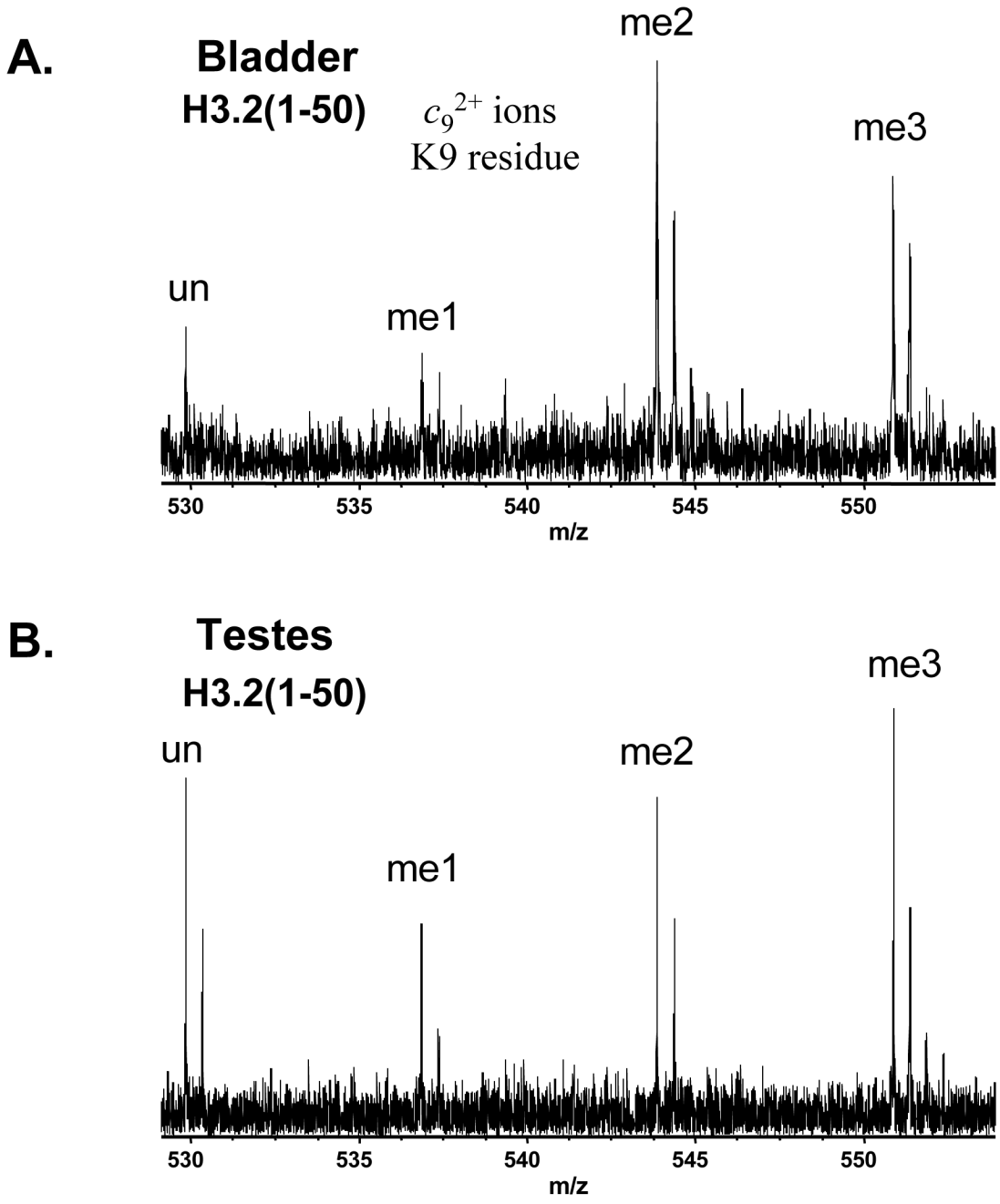

Figure 4.

Zoom region from ECD spectra of the histone H3.2(1-50) polypeptide from the +8 precursor species showing the c_9^{2+} fragment ions corresponding to posttranslational modifications on the K9 residue (528-552 *m/z* region) from rat (**A.**) bladder and (**B.**) testes tissue samples. Clear differences in the degree of methylation at K9 between both samples can be seen with the testes H3.2 sample containing higher levels of both unmodified K9 and K9me3.

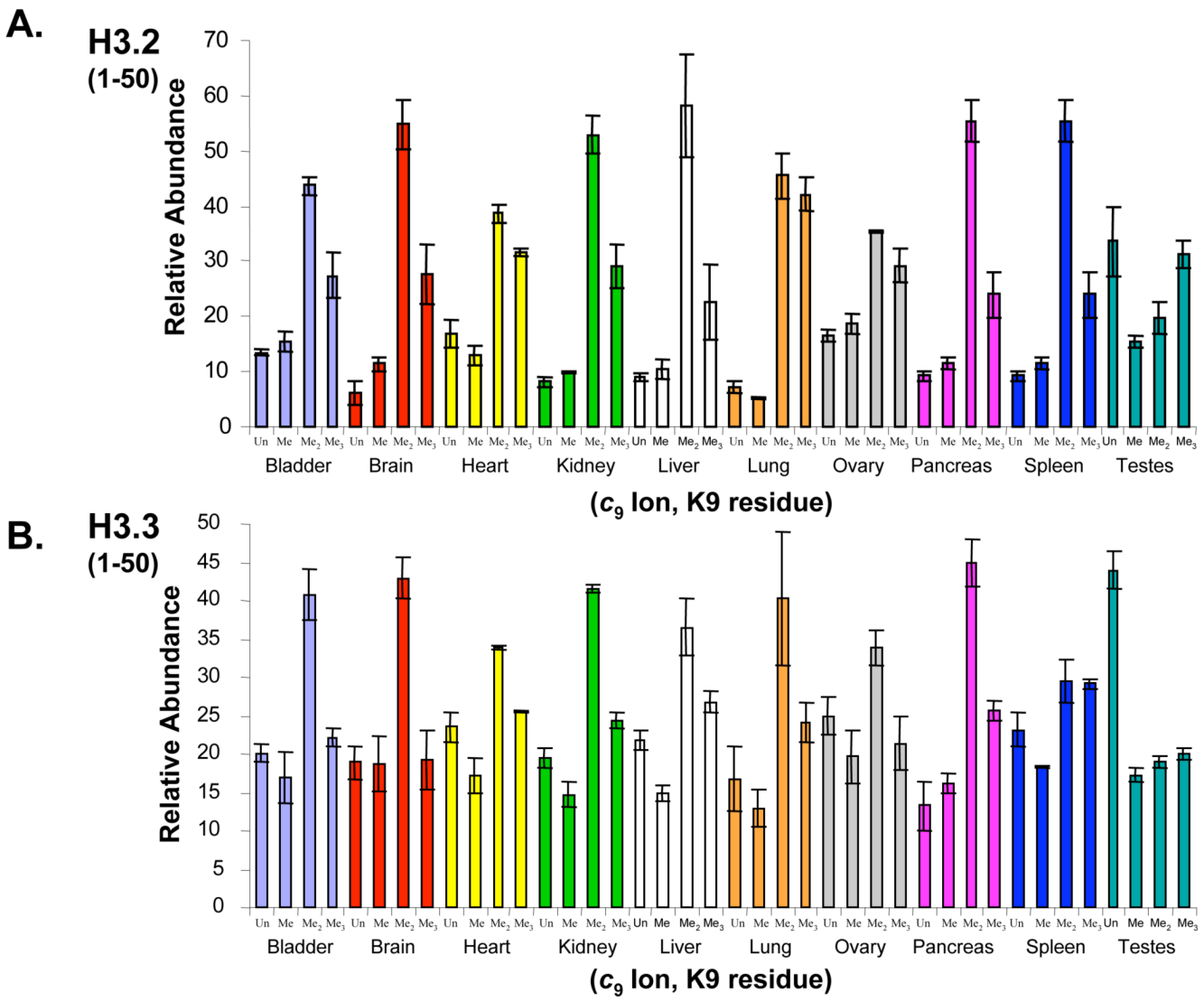

Figure 5.

Histograms showing the comparison of K9 modifications (unmodified, mono-, di- and trimethylation) observed in ECD generated c_9^{2+} ions (FIRRs) from the (**A.**) H3.2(1-50) and (**B.**) H3.3(1-50) polypeptides for all ten rat tissues as labeled. Fractional occupancy was determined from ECD spectra produced from the 8+ charge state species. Histograms depict the average of three independent biological samples (N=3) and standard deviations are shown as error bars.

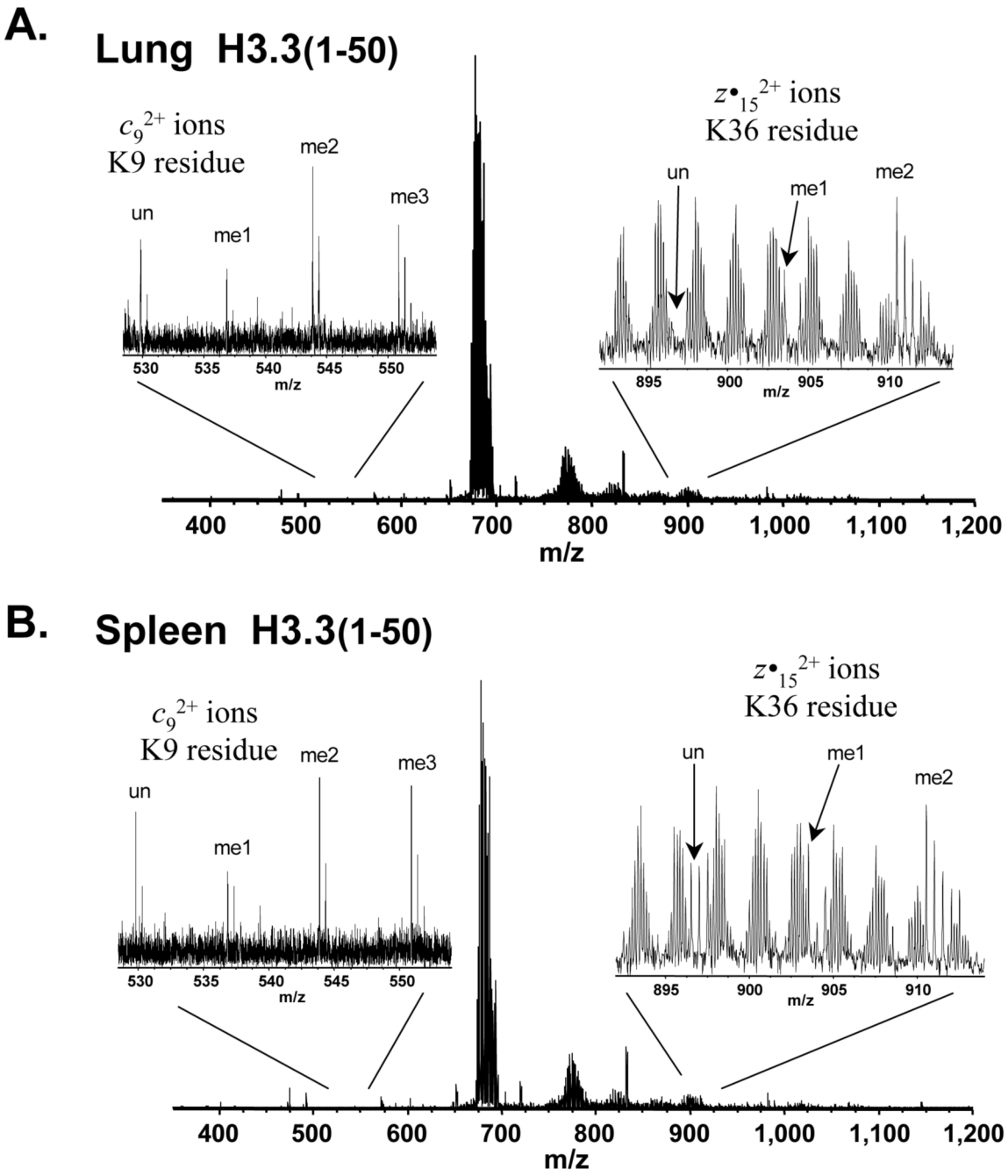

Figure 6.

Comparison of ECD spectra generated from the histone H3.3(1-50) polypeptide prepared from different rat tissues. **A.** ECD fragmentation of the H3.3(1-50) 8+ charge state species from rat lung. **B.** ECD fragmentation of the H3.3(1-50) 8+ charge state species from rat spleen. Zoom regions spanning 528-552 *m/z* and 895-912 *m/z* in both spectra display fragment ions which correspond to modifications on K9 (unmodified, mono-, di- and trimethylation) and K36 (unmodified, mono- and dimethylation), respectively. The largest PTM differences between the samples are found to be at the levels of K9me3 and unmodified K36.

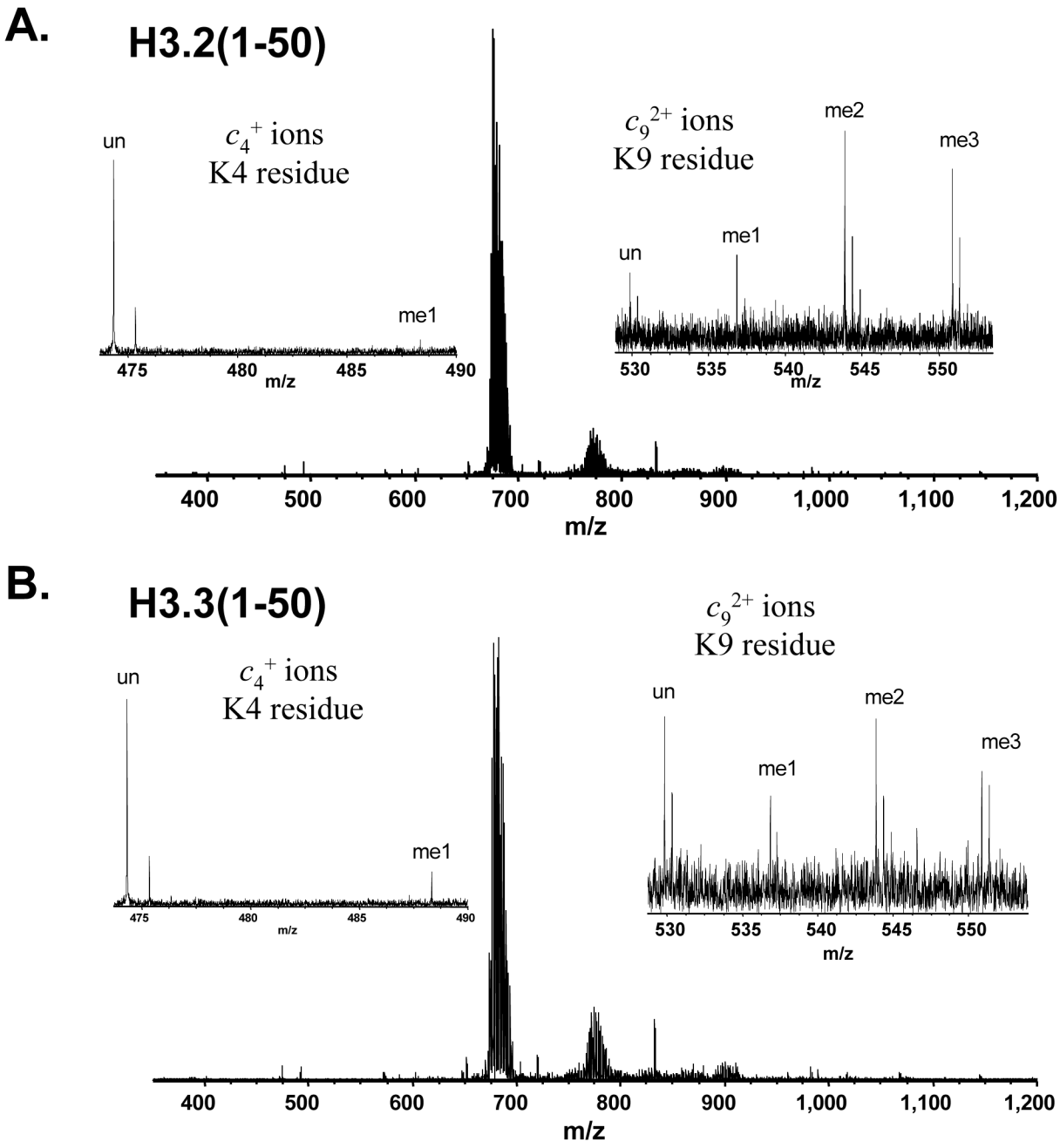

Figure 7.

Differences in posttranslational modifications between histone H3 variants extracted from heart tissue. ECD fragmentation of the 8+ charge state species from the (**A.**) H3.2(1-50) and (**B.**) H3.3(1-50) polypeptides. Zoom regions in the mass spectra spanning 474-490 *m/z* and 528-552 *m/z* in both spectra display fragment ions which correspond to modifications on K4 (monomethylation) and K9 (unmodified, mono-, di- and trimethylation), respectively. Overall, H3.3 contained a higher level of K4me1, while K9 methylation was slightly higher (as noted by less unmodified K9 species) on histone H3.2.

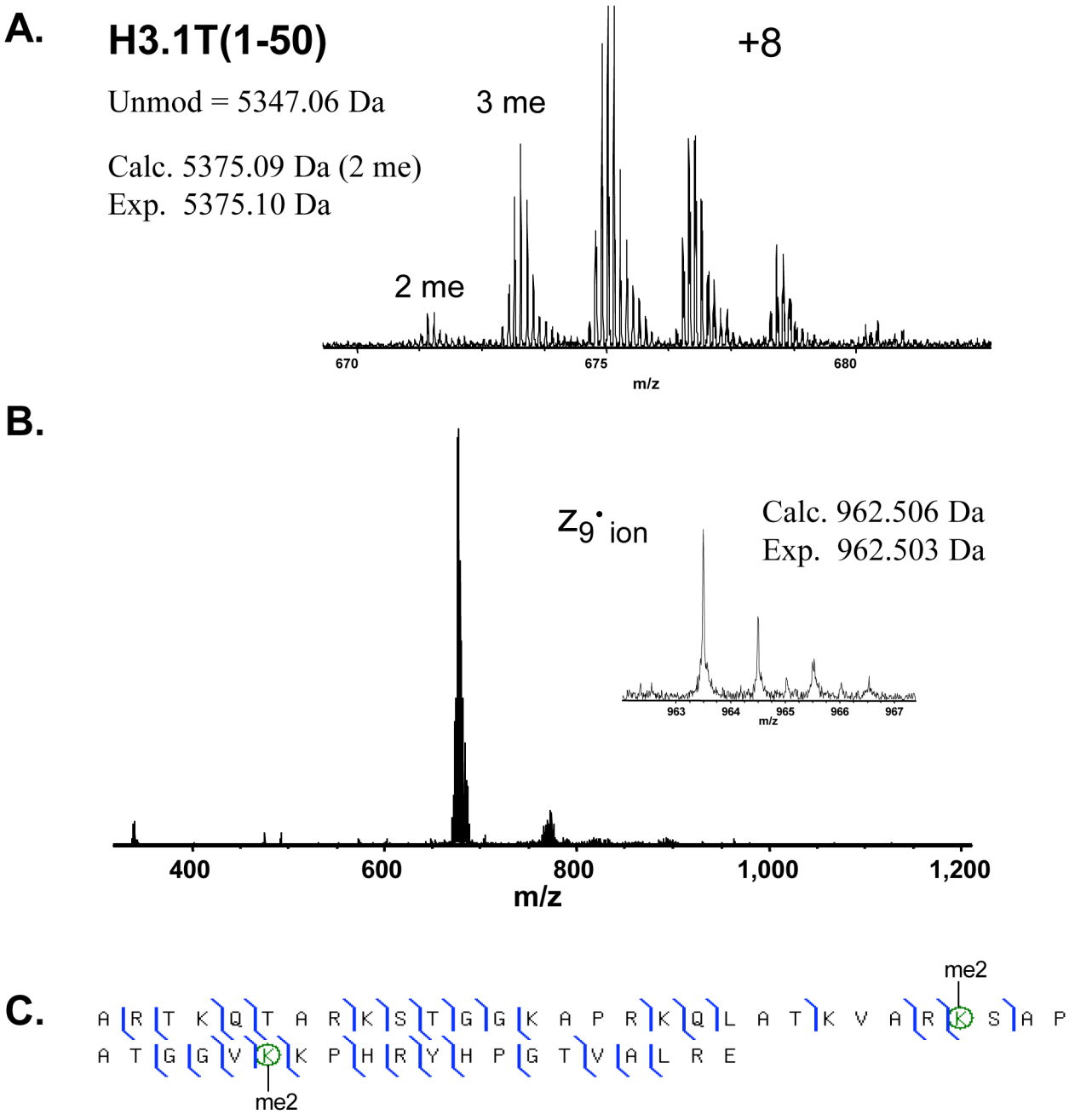

Figure 8.

Characterization of a novel rat testes-specific H3 isoform (H3.1T). **A.** Broadband mass spectrum of the 8+ charge state of the 1-50 fragment isolated from the third histone H3 RP-HPLC peak (see Supplemental Figure 1I) of acid-extracted material from rat testes. The first peak was found to be at 5375.10 Da, followed by peaks separated by approximately 14 Da. **B.** ECD fragmentation of the 8+ charge state species isolated in (**A.**). Zoom regions in the mass spectra shows the fragment $z^{\bullet +}_9$ ion that indicates that a R H substitution is found in this H3 protein. **C.** ECD fragment map generated from the fragmentation spectrum shown in (**B.**) showing that a novel histone H3.1-like molecule is expressed in the testes. The H3 protein

sequence that fit the ECD spectrum was entered in the NCBI database as ‘predicted: similar to H3 histone family member’ (accession # XP_220509).